Agricultural and Forest Meteorology 339 (2023) 109578

Contents lists available at ScienceDirect

Agricultural and Forest Meteorology

journal homepage: www.elsevier.com/locate/agrformet

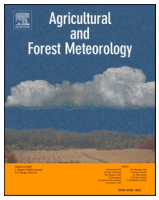

# $CH_4$ emissions from a double-cropping rice field in subtropical China over seven years

Xiao Liu [a,b], Xiaoqin Dai [a,*], Fengting Yang [a], Shengwang Meng [a], Huimin Wang [a,b,*]

[a] Qianyanzhou Ecological Research Station, Key Laboratory of Ecosystem Network Observation and Modeling, Institute of Geographic Sciences and Natural Resources Research, Chinese Academy of Sciences, Beijing 100101, China
[b] College of Resources and Environment, University of Chinese Academy of Sciences, Beijing 100190, China

ARTICLE INFO

*Keywords:*
$CH_4$ flux
Double rice
Eddy covariance
Long-term observation

ABSTRACT

Rice paddies are important sources of the greenhouse gas methane ($CH_4$). However, it is difficult to precisely quantify $CH_4$ emissions using the static chamber method because of their discontinuous measurements as well as the spatial and temporal variability of $CH_4$ emissions. To precisely quantify $CH_4$ emissions from rice paddies and gain deep insight into the emission rhythm and environmental effects, a seven-yearlong $CH_4$ flux measurement was carried out continuously using the eddy covariance method in a double cropping rice paddy in subtropical China. The annual $CH_4$ emissions were $42 \pm 2$ g C $m^{-2}$. The half hourly $CH_4$ flux was highly correlated with gross primary production (GPP) and environmental factors, such as soil temperature (Ts), and latent heat flux (LE), which explain 47–91% of the $CH_4$ diurnal variation. However, the peak of $CH_4$ generally appeared at dusk during the vigorous growth period, which was quite different from the GPP peak around noon. $CH_4$ flux seasonal dynamic were more complex, with double peaks during the growing season and lower values during the fallow season. Interestingly, in contrast to previous studies of linear or exponential relationships with short-term datasets, daily $CH_4$ and GPP showed a logarithmic relationship at the vegetative stage in this study with seven-year data, this is crucial in improving the model accuracy in estimating annual $CH_4$ emissions. The result implies that long-term observation is necessary to accurately assess $CH_4$ emissions from rice paddy.

## 1. Introduction

Methane ($CH_4$) is an important greenhouse gas, second only to $CO_2$, with a global warming potential is 28 times higher than that of $CO_2$ over a 100-year period (Kim et al., 2016). Its concentration has increased from 720 ppb to 1850 ppb since 1750 (Etheridge et al., 1998), and has had a significant influence on the global atmospheric temperature (Alberto et al., 2014; Nisbet et al., 2019). Rice paddies are one of the largest anthropogenic sources of atmospheric $CH_4$, accounting for approximately 12% of the global $CH_4$ emissions (IPCC, 2007). The sown areas of rice in China account for 18% of the world, but production accounts for 28% of that of the world (FAO, 2020). Double rice is the dominant cropping system in southern China, accounting for 33% of the rice-planting area in China (NBS, 2018). Double rice paddies have higher $CH_4$ emissions than single rice paddies (Feng et al., 2013; Jiang et al., 2018). However, the annual $CH_4$ emissions varied greatly based on short-term discontinuous observations using the chamber method because of the complicated effects of environmental variables (Chaichana et al., 2018). Quantifying the annual emissions of $CH_4$ from rice paddies and understanding their emission mechanisms are critical for agricultural management to mitigate climate change.

The release of $CH_4$ from the soil is the net sum of a mix of processes including production, oxidation, and transportation (Le Mer and Roger, 2001). $CH_4$ is generally produced by methanogens under anaerobic soil conditions (Conrad, 2002; Ge et al., 2018), which are controlled by substrates, nutrient inputs, soil water, and temperature; its role has been widely documented (Li et al., 2018; Tariq et al., 2017a, 2017b). Simultaneously, $CH_4$ is oxidized by methanotrophs under aerobic conditions (Wassmann and Aulakh, 2000). The remaining $CH_4$ is transported to the atmosphere via ebullition, diffusion, and plant aerenchyma (Neue, 1993). However, there is considerable uncertainty in the precise evaluation of $CH_4$ emissions from rice paddies owing to their complexity (Chaichana et al., 2018; Tariq et al., 2017b).

Plants are one of the most important factors influencing $CH_4$ flux because they provide carbon substrates for methanogens to control $CH_4$ production (Bhattacharyya, 2019; Chen et al., 2019). Many studies have

* Corresponding authors.
*E-mail addresses:* daixq@igsnrr.ac.cn (X. Dai), wanghm@igsnrr.ac.cn (H. Wang).

https://doi.org/10.1016/j.agrformet.2023.109578
Received 2 March 2023; Received in revised form 19 June 2023; Accepted 21 June 2023
Available online 8 July 2023

indicated that the emission rate of $CH_4$ was tightly related with gross primary production (GPP) in an exponential or linear manner in rice paddies (Chen et al., 2020; Dai et al., 2019; Li et al., 2019; Song et al., 2015), implying that the $CH_4$ flux increases at a stable or accelerated rate with increasing GPP. These relationships have even been embedded into models for evaluating $CH_4$ emissions from rice paddies, such as the iPEACE model (Ueyama et al., 2022), Peatland-VU (Mi et al., 2014), PEPRMT-TPGPP model (Oikawa et al., 2017), and the process-based model by Kettunen (2003). Therefore, the accurately understanding the relationship between $CH_4$ and GPP is of paramount importance for evaluating $CH_4$ emissions from rice paddies. We also noticed that most relationships between $CH_4$ emissions and GPP were established based on a short-term dataset. Studies indicated that over long periods of time can reveal the influence caused by large environment variations that are difficult to reveal in short term (Hanson and Walker, 2020), and models fitted with $CH_4$ estimates based on short-term data (e.g., one or two years) are unstable (Ueyama et al., 2022). Therefore, further studies should be conducted using long-term datasets.

The well-documented environment driving forces of $CH_4$ emissions mainly include temperature, soil moisture, and air pressure (Feng et al., 2013; Kim et al., 2016; Wang et al., 2016). Temperature is often treated as the primary driver of carbon fluxes as it controls the available energy (Mitra et al., 2020), which causes different diurnal patterns of $CH_4$ flux (Chen et al., 2019; Ge et al., 2018). Additionally, it controls microbial processes that produce and consume $CH_4$ (Liu et al., 2022). Many previous studies have indicated that as soil moisture increases, oxygen concentrations can decrease, which promotes anaerobic conditions and $CH_4$ production, and vice versa (Dai et al., 2019; Rinne et al., 2018). The anaerobic and aerobic soil zones are influenced by soil moisture, which adjusts the balance between $CH_4$ production and oxidation. Air pressure (PA) as a trigger for $CH_4$ ebullition is direct driver of $CH_4$ transport (Knox et al., 2020). Several studies have investigated the influence of PA itself as well as changes in PA, hypothesizing that more bubbles filled with $CH_4$ will form when the pressure suddenly drops (Morin, 2019).

The annual $CH_4$ emissions of double rice had been widely reported but the values vary greatly from 17 g $m^{-2}$ to 95 g $m^{-2}$ in the south and central of China (Chen et al., 2021; Feng et al., 2021; Wang et al., 2019; Yang et al., 2018; Yu et al., 2021), even though the environment, agricultural management, and cropping system were similar in many cases. We also noticed that most results for $CH_4$ flux in rice paddies were obtained using the closed static chamber method.

The closed static chamber method is generally used for $CH_4$ flux measurements. However, it is difficult to reflect the real situation of $CH_4$ emissions because its measurement area is generally less than 1 $m^2$, and it is hard to measure $CH_4$ pulses caused by rain, strong winds, fertilization, etc. due to a discontinuous measurement. A simple linear fill-in approach would further increase the uncertainty of $CH_4$ emissions if the fluxes were upscaled to large spatial and temporal scales (Jauhiainen et al., 2005; Maier et al., 2019; Yu et al., 2013; Yuan et al., 2016; Zhao et al., 2019). The limitations of this method may also partially contribute to the result discrepancy.

The development of EC technology has enabled the continuous measurement $CH_4$ fluxes at a high frequency of 10 Hz on an ecosystem scale (Alberto et al., 2014; Yu et al., 2013). At present, the eddy covariance method is mainly used to study ecosystem-scale nocturnal $CH_4$ flux from rice fields, $CH_4$ emissions during the non-growing season (Reba et al., 2019), and $CH_4$ pulses triggered by rainfall, fertilization, and other disturbances (Iwata et al., 2018). The eddy covariance method compensates for the shortcomings of the static chamber method, such as its small measurement area, discrete time and inability to measure $CH_4$ pulses.

$CH_4$ flux measurements based on eddy correlation began in the 1990s (Verma et al., 1992), but continuous observations have only been made since the 2010s. However, $CH_4$ emissions reported in rice paddies using the EC method are mainly based on short datasets, such as one or two years from rice paddies (Ge et al., 2018; Iwata et al., 2018; Li et al., 2018; Meijide et al., 2017). Currently, there are only a few studies with observation period beyond the 1–2 years (Hwang et al., 2020; Knox et al., 2016; Runkle et al., 2019). Previous studies have indicated the importance of long-term data on the precision of $CH_4$ estimation model because of the large interannual environmental variations, and a long-term data set of at least three years or more is necessary (Morin, 2019; Ueyama et al., 2023, 2022).

In this study, seven-yearlong $CH_4$ flux measurements were conducted in a double rice paddy in subtropical China. Our main objectives were (1) to quantify the annual $CH_4$ emissions, their interannual variation and driving forces for double rice paddy, and (2) to analyze the seasonal variation of $CH_4$ flux and test its relationship with GPP using long-term observation data.

## 2. Materials and methods

### 2.1. Study site

The experiment was carried out at the National Qianyanzhou Critical Zone Observatory of the Red Soil Hilly Region (26°44′48″N, 115°04′13″E), located in Jiangxi Province in subtropical China, which belongs to China Flux Observation and Research Network. The region has a subtropical monsoon climate, with a drought season generally from July to September and a rainy season from April to June. The mean annual temperature is 19.4°C, and the mean annual precipitation is approximately 1463 mm. The soil is a typical red soil and is classified as an Ultisol in the USDA soil taxonomy. The parent material of the soil consists of red sandstone and sandy conglomerates. The topsoil consists of 17% clay (<0.002 mm), 25% silt (0.002–0.02 mm) and 56% sand (0.02–2 mm) (Dai et al., 2016). The soil pH was 4.97, and the bulk density was 1.29 g $cm^{-3}$. The main cropping system in this region is double rice.

### 2.2. Rice paddy management

Rice was cultivated following a conventional double-rice cropping system with early rice from late March to July, late rice from late July to November, and a fallow period from November to the next March (Table 1). The rice varieties for both early and late rice, purchased from the local market, were different every year. But their theoretical yields were quite similar and relatively high among cultivars in the same growing season. At the start of each growing season, the paddy was prepared by irrigation and harrowing, which incorporated weed and straw residues from the previous rice crop, leveling, and fertilization. Early rice was direct-seeded at a rate of 75 kg $ha^{-1}$ (approximately 4000,000 seeds $ha^{-1}$), and late rice was transplanted at a density of 235,000 hills $ha^{-1}$ with a 20-day-old rice seedling soon after the harvest of early rice in mid-July. The fertilizers were applied twice during each growing season. Compound fertilizers and urea were applied as basal fertilizers at the rates of 56 kg N $ha^{-1}$, 24 kg P $ha^{-1}$, 46 kg K $ha^{-1}$ and 78 kg N $ha^{-1}$, 34 kg P $ha^{-1}$, 65 kg K $ha^{-1}$ before seeding for early rice, and transplanting for late rice, respectively. At the tillering stage of early rice and late rice, 100 kg N $ha^{-1}$, 8 kg P $ha^{-1}$, and 15 kg K $ha^{-1}$ were applied to the paddy. The rice was harvested using a combine harvester which returned all the rice residues to the paddy.

An intermittent irrigation regime (drainage mostly during the late tillering, panicle, and ripening stages) was applied for rice paddies during both seasons (Shao et al., 2017). Early rice was continuously flooded for an average of 70 days, while late rice was continuously flooded for an average of 40 days. The drainage was conducted for early rice in the late tillering period because of the abundant rainfall.

### 2.3. Fluxes and environment measurement

An open-path eddy covariance flux system was set up to measure $CH_4$ and $CO_2$ fluxes in the center of a rice paddy with an area of 1.43 ha (130

**Table 1**
Dates encompassing the different growth stages of early rice and late rice from 2013 to 2020.

| | | 2013 | 2015 | 2016 | 2017 | 2018 | 2019 | 2020 |
|---|---|---|---|---|---|---|---|---|
| Early rice | Plant date | 24 Mar | 26 Mar | 26 Mar | 27 Mar | 24 Mar | 8 Apr | 7 Apr |
| | Harvest date | 13 July | 12 July | 12 July | 16 July | 14 July | 17 July | 16 July |
| | Seedling days | 32 | 30 | 34 | 31 | 33 | 22 | 31 |
| | Tillering days | 29 | 22 | 25 | 23 | 28 | 28 | 21 |
| | Booting days | 21 | 30 | 23 | 24 | 22 | 16 | 17 |
| | Ripening days | 30 | 27 | 27 | 33 | 31 | 35 | 32 |
| | grain yield (t $ha^{-1}$) | 6.3 | 6.41 | 6.65 | 6.44 | 5.43 | 6.74 | 6.0 |
| Late rice | Plant date | 14 July | 13 July | 13 July | 17 July | 15 July | 18 July | 17 July |
| | Harvest date | 3 Nov | 26 Oct | 7 Nov | 6 Nov | 31 Oct | 28 Oct | 5 Nov |
| | Seedling days | 22 | 22 | 23 | 22 | 22 | 20 | 23 |
| | Tillering days | 22 | 24 | 26 | 27 | 27 | 29 | 30 |
| | Booting days | 22 | 21 | 20 | 20 | 19 | 21 | 20 |
| | Ripening days | 47 | 39 | 49 | 45 | 41 | 33 | 39 |
| | grain yield (t $ha^{-1}$) | 7.53 | 5.69 | 6.58 | 6.06 | 7.88 | 8.37 | 6.89 |

Note: Due to the damage of the instrument, the year "2013" is defined as the period from July 2012 to July 2013 in this paper.

m × 110 m) on 14 July 2012. However, the system was damaged by a lightning strike, and data were lost from mid-July 2013 to December 2014. The year "2013" is defined as the period from July 2012 to July 2013. Thus, the data for seven years were reported here (Table 1).

The EC flux system consisted of an open-path $CH_4$ infrared gas analyzer (LI-7700, Li-COR Inc., USA), an open-path $CO_2/H_2O$ infrared gas analyzer (LI-7500, Li-COR Inc., USA), and a three-axis sonic anemometer (CSAT3, Campbell Scientific Inc. (CSI), USA). The system was set up at a height of 2.5 m, approximately 1.5 m above the canopy. Fluctuations in the $CH_4$ and $CO_2/H_2O$ concentrations, air pressure (PA), and vertical wind speed (Ws) were detected at a frequency of 10 Hz and recorded using a datalogger (CR5000, CSI). $CO_2$ and $CH_4$ fluxes were calculated as the covariance of $CO_2$ or $CH_4$ concentration and vertical wind velocity in 30 min, and the raw flux data were post-processed and quality controlled using EddyPro 6.1.1 software (LI-COR), in which the double rotation, block average (Moncrieff et al., 2004), density fluctuations (WPL correction) (Webb et al., 1980), spectral corrections (Moncrieff et al., 2004, 1997), sonic virtual temperature correction (Van Dijk and Han Dolman, 2004), and the incorporated frequency response correction (Massman and Lee, 2002) were carried out. Footprint estimation using the method of Kljun et al. (2004) showed that 90% of the measured eddy flux came from within 67 ± 45 m during daytime and 63 ± 27 m during nighttime.

Parallel to the flux measurements, some meteorological parameters were measured. Net radiation (Rn) and downward solar radiation (DR) were measured using a four-component radiometer (NR01, Hukseflux, Delft, Netherlands). Photosynthetic photon flux density (PPFD) was measured using a quantum sensor (LI-190SB, LI-COR). Air temperature (Ta) and relative humidity (RH) were measured using a hydrothermal sensor (HMP45C, CSI). Soil temperature (Ts) at a depth of 10 cm was measured using a type-E thermocouple burial probe (105E-L, CSI), and soil moisture (Sm) was measured using a soil moisture sensor (CS616-L, CSI). These data were automatically recorded using a data logging system. Precipitation was monitored using a rain gage (52,203, RM Young Inc.).

## 2.4. Gap filling

### 2.4.1. $CH_4$ flux

The half-hour data gaps of the $CH_4$ flux were 55.2% during the observation period, and the raw flux data were removed when rainfall, instruments malfunction, low data quality, and friction wind speed (u*) values were less than 0.1 m $s^{-1}$ at nighttime. To calculate the annual $CH_4$ emissions from rice paddy, flux data gaps were filled with the interpolation method. The marginal distribution sampling (MDS) method, multiple imputation (MI) method, and artificial neural networks (ANN) method may exhibit overfitting or false correlations between $CH_4$ fluxes and meteorological factors owing to the fitting process (Dai et al., 2019). We filled the gaps in $CH_4$ fluxes using the mean diurnal variation (MDV) method. The data were first divided into nine groups according to the rice growth stage in each year. Then, the data gaps were interpolated in groups as follows: (1) gaps shorter than 2 h were filled by a simple linear interpolation method; (2) gaps longer than 2 h were filled by a MDV procedure (Chaichana et al., 2018), except for the big gap from July 2013 to December 2014. The coefficient of determination between the simulated values and the observed values is between 0.7 and 0.9, and the RMSE (root mean square error) is relatively concentrated between 0.5 and 0.8 in different years. These results indicate that the MDV method could be used for $CH_4$ flux gap-filling.

### 2.4.2. $CO_2$ flux

Gaps in NEE were filled at different growth stages following the method proposed by Falge et al. (2001): (1) gaps shorter than 2 h were filled using a simple linear interpolation method; (2) the gaps longer than 2 h were filled using eq(1) for nighttime and eq(2) for daytime. The gap-filled nighttime NEE was used to evaluate *Re*. The GPP was calculated by subtracting gap-filled NEE from *Re* using eq (3). Negative NEE values indicate net $CO_2$ uptake, whereas positive values indicate net $CO_2$ release. Both GPP and *Re* were positive. The parameters for the different stages and years are listed in Table S1.

At nighttime, missing NEE data were gap-filled with air temperature (Lloyd and Taylor, 1994).

$$NEE = Re = a \exp(b\ Ta) \tag{1}$$

where a and b are two empirical coefficients.

At daytime, missing NEE data were gap-filled as follows with PPFD (Falge et al., 2001).

$$NEE = -\frac{\alpha\beta PPFD}{\alpha PPFD + \beta} + Re \tag{2}$$

where $\alpha$ is the apparent quantum yield, $\beta$ is the maximum $CO_2$ flux at infinite light level.

At daytime, GPP data were calculated as follows (Baldocchi et al., 2015).

$$GPP = Re - NEE \tag{3}$$

### 2.4.3. Other factors

There were gaps in environmental factors, they were filled using a simple linear interpolation method with gaps shorter than 2 h. For gaps longer than 2 h, a linear fit was performed with data from a nearby eddy covariance system to provide missing data. Daily environmental factors were calculated using the gap-filled environmental factors. Yield-scaled $CH_4$ emissions represented the $CH_4$ emissions per unit rice grain yield (kg), which were used to evaluate the comprehensive impacts of cropping practices on $CH_4$ emissions and rice yields (Feng et al., 2013).

### 2.5. Data analysis

The relationships between $CH_4$ flux and plant and environmental factors (NEE, *Re*, GPP, PPFD, Rain, Ta, Ts, RH, VPD, Ws, Sm, DR, Rn, LE, PA) were analyzed using Pearson correlation on a diurnal scale for different growth stages. All-subset regression statistics were used to solve the collinearity problem (Leamer, 1985). We used generalized linear model to investigate the factors controlling $CH_4$ flux at the diurnal time scale. Relative weights were used to assess the relative importance of drivers in the models (Kabacoff, 2015). We also investigated the time lag by a lag coupling between $CH_4$ flux and GPP or Ts at the diurnal scale following Rinne et al. (2018). Random forest was used to rank the factors in order of importance on the seasonal scale based on the increase in mean square error (%IncMSE) (Liaw and Wiener, 2002; Liu et al., 2021). Linear and non-linear regressions were used to test the relationships between $CH_4$ flux and GPP, Ts, air pressure, and soil moisture on seasonal and annual scale. The AIC value was used to compare the precision of the linear, exponential, logarithmic, and polynomial models of the relationships between $CH_4$ emissions and GPP during the vegetative stage (Ehnes et al., 2011). Best-fitting regression models are presented. All analyses were done using R 4.2.1.

## 3. Results

### 3.1. Diurnal dynamics of $CH_4$ flux and its dominant driving forces

The mean diurnal $CH_4$ flux varied from 0.04 to 0.38 μmol $m^{-2}$ $s^{-1}$ for the growing period of early rice, 0.01 to 0.66 μmol $m^{-2}$ $s^{-1}$ for the growing period of late rice, and −0.001 to 0.033 μmol $m^{-2}$ $s^{-1}$ for the fallow period from 2013 to 2020 (Fig. 1). The $CH_4$ flux peak mostly occurred from afternoon to dusk in the growing stages. No clear diurnal dynamics of $CH_4$ flux were observed during the fallow period when $CH_4$ flux was very low.

The dominant forces driving $CH_4$ emissions during the growing stages were GPP and Ts. In addition, some other environmental factors, such as wind speed, LE, and VPD, also affected $CH_4$ to some extent in certain growing stages, with $r^2$ of models in growing stages ranging from 0.64 to 0.91 (Table 2 & Fig. S1). During the seedling stages of early rice and late rice, the relative importance of LE and Ts was higher than that of GPP (Table S2), as the relative weights of GPP were less than 21% in the models. During other stages of growing season, GPP had highest relative weights in models, ranging from 41% to 83% (Table S2). During the fallow season, NEE and Ts dominated $CH_4$ emissions ($r^2$ = 0.47) (Table 2 and Fig. S1), and the relative weights of NEE was 89% (Table S2).

A hysteretic relationship between $CH_4$ flux and GPP across different stages was observed in diurnal scale (Fig. 2), as the peak $CH_4$ flux did not match the two dominant drivers. At the same growth stages of early rice and late rice, $CH_4$ flux and GPP showed similar lag times (Fig. 2a). During the fallow season, variations in $CH_4$ flux shared most of the information with GPP with a time lag of 0.5 h. At the seedling stage, there was virtually no lag time between $CH_4$ flux and GPP. The lag time between $CH_4$ flux and GPP was approximately 4 h at the tillering stage. During the booting and ripening stages, the lag time between $CH_4$ flux and GPP lasted approximately 1.5 h. The lag correlations between $CH_4$ flux lag and Ts were significant with the lag times changing at different stages (Fig. 3b). And the lag times between $CH_4$ flux and Ts were 0 h at seedling stage, nearly 4.5 h at tillering stage, and nearly 2.5 h at booting and ripening stages.

**Table 2**
Generalized linear Models at Diurnal Scale, Their Equation, Adj. $R^2$(Adjusted $R^2$).

| Period | Equation model | Adj. $R^2$ |
|---|---|---|
| ER-seedling | $F_{CH4}$=−0.012GPP+0.006Ts+0.0004LE-0.023 | 0.64 |
| ER-tillering | $F_{CH4}$=−0.019GPP +0.02Ts+0.002LE-0.316Ws+0.066 | 0.85 |
| ER-booting | $F_{CH4}$=−0.001GPP+0.017Ts+3.704Sm-1.743 | 0.64 |
| ER-ripening | $F_{CH4}$=−0.005GPP+0.007Ts+2.984Sm+0.044VPD-1.319 | 0.69 |
| LR-seedling | $F_{CH4}$=−0.017GPP+0.012 Ts +0.001LE +0.033 | 0.91 |
| LR-tillering | $F_{CH4}$=−0.015GPP+0.01Ts+0.001LE +0.138 | 0.86 |
| LR-booting | $F_{CH4}$=−0.005GPP+0.016Ts-0.241 | 0.74 |
| LR-ripening | $F_{CH4}$=−0.004GPP+0.01Ts-0.15 | 0.64 |
| Fallow season | $F_{CH4}$=0.003NEE+0.002Ts-0.012 | 0.47 |

Note. ER, early rice; LR, late rice; $F_{CH4}$, $CH_4$ flux (μmol $m^{-2}$ $s^{-1}$); GPP, gross primary production (μmol $m^{-2}$ $s^{-1}$); NEE, net ecosystem exchange (μmol $m^{-2}$ $s^{-1}$); Ts, soil temperature in 10 cm (°C); LE, latent heat flux (W $m^{-2}$); Ws, wind speed (m $s^{-1}$); Sm, soil moisture of volumetric water content ($cm^3$ $cm^{-3}$); VPD, vapor pressure deficit (kPa). All results were highly significant ($p < 0.001$).

### 3.2. Seasonal dynamics of $CH_4$ flux and its dominant driving forces

The $CH_4$ flux showed strong seasonal variations with double peaks appearing during the growing season. The $CH_4$ peak value varied from 0.4 g C $m^{-2}$ $d^{-1}$ to 1.23 g C $m^{-2}$ $d^{-1}$ during the 7 years (Fig. 3), and tends to be increased year by year for the late rice, but the peak variation trend of the early rice was not clear (Fig. 3). The $CH_4$ emissions were close to zero during the fallow season, gradually increased from the beginning of the growing season of early rice, and rose to the first peak at the end of flooding. With drainage and harvest, the daily $CH_4$ emissions gradually decreased to near zero, followed by the planting, growth, and harvest of the late rice, and the second $CH_4$ peak appeared in the vigorous growth stage (Fig. 3).

During the vegetative stage before mid-season drainage, $CH_4$ flux

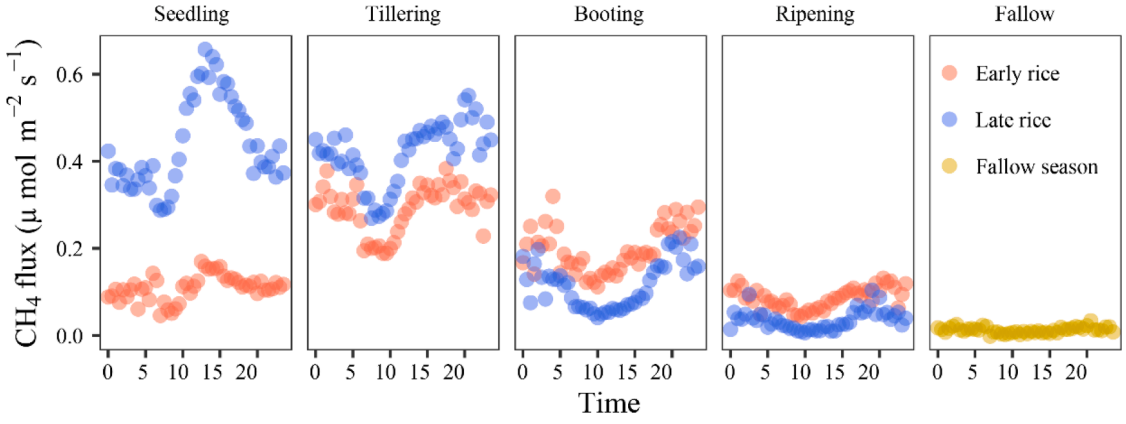


**Fig. 1.** Mean diurnal variation in $CH_4$ flux during the growing season of early rice (red), late rice (blue), and fallow season (yellow) across all years. The mean diurnal $CH_4$ flux was calculated using qualified half-hourly flux data without gap filling.

**Table 3**
Importance of significant predictors of the $CH_4$ flux in seasonal scale by Random Forest analysis.

| Stage | Increase in mean square error (%) | | | | | | | | | | | | | | $R^2$ |
|---|---|---|---|---|---|---|---|---|---|---|---|---|---|---|---|
| | DR | GPP | LE | NEE | PA | PAR | *Re* | RH | Rn | Sm | Ta | Ts | VPD | Ws | |
| ER Seedling | 2.37 | 12.47** | 5.85 | 3.71 | 19.87** | 4.59 | 12.14** | 2.37 | 2.49 | 15.11** | 9.66* | 19.92** | 4.57 | 0.71 | 0.61 |
| ER Tillering | 4.74 | 15.69** | 6.63 | 11.61** | 9.03** | 3.77 | 16.17** | 6.88 | 2.15 | 16.95** | 15.95** | 7.76 | 5.19 | 2.55 | 0.44 |
| ER Booting | 7.49** | 9.39** | 6.20 | 5.64 | 5.06 | 4.65 | 6.28* | 15.27** | 6.48* | 44.55** | 11.81** | 5.49 | 12.73** | 2.95 | 0.75 |
| ER Ripening | 6.40 | 12.02* | 12.05** | 18.62** | 9.37* | 5.95 | 7.66 | 4.48 | 5.28 | 11.03** | 6.35 | 7.35 | 6.17 | 3.43 | 0.39 |
| LR Seedling | 5.76 | 18.11** | 10.46** | 11.55** | 4.78 | 6.48* | 12.45** | 6.35 | 4.96 | 29.62** | 5.82 | 6.42* | 6.58* | 2.03 | 0.66 |
| LR Tillering | 5.42 | 7.28 | 4.43 | 12.22** | 14.27** | 10.24* | 12.79** | 9.19** | 7.67 | 36.80** | 8.61** | 9.06* | 10.87** | 3.70 | 0.7 |
| LR Booting | 4.80 | 5.76 | 4.51 | 4.84 | 5.15 | 5.75 | 7.97 | 4.07 | 4.14 | 37.27** | 5.82 | 6.71* | 3.47 | 0.40 | 0.51 |
| LR Ripening | 7.16 | 9.99 | 9.07 | 6.38 | 16.26** | 5.67 | 6.83 | 7.99 | 4.83 | 22.65** | 11.39* | 13.03** | 5.72 | 1.06 | 0.53 |
| Fallow | 9.99 | 5.53 | 9.27 | 7.49 | 6.13 | 7.75 | 12.59 | 8.66 | 8.48 | 22.56** | 10.84 | 12.41 | 9.79 | 2.47 | 0.27 |

Note. ER, early rice; LR, late rice. Predictors include soil moisture (Sm), respiration (*Re*), air pressure (PA), gross primary production (GPP), soil temperature (Ts), air temperature (Ta), net ecosystem exchange (NEE), evapotranspiration (ET), latent heat flux (LE), vapor pressure deficit (VPD), relative humidity (RH), direct solar radiation (DR), photosynthetic photon flux density (PPFD), net radiation (Rn), wind speed (Ws). The * and ** sign indicate the significance in $p < 0.05$ and significance in $p < 0.01$, respectively.

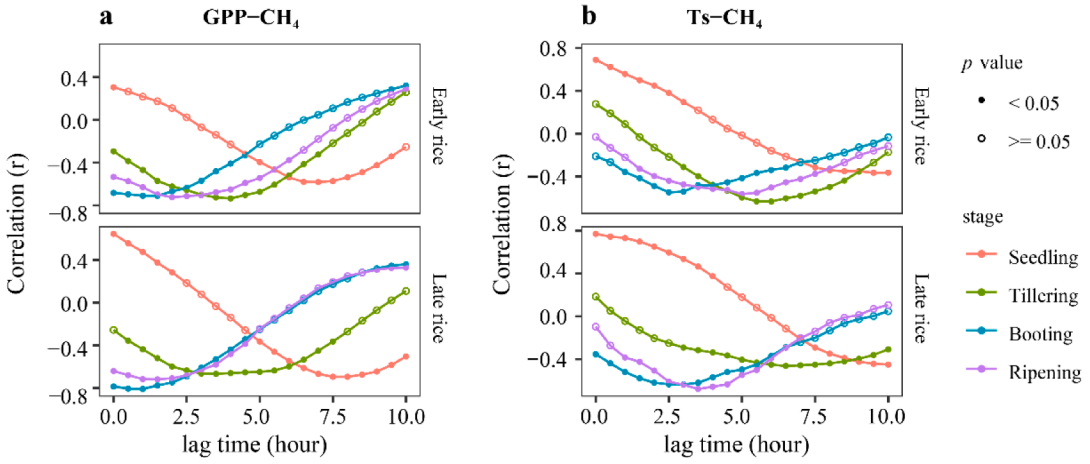


**Fig. 2.** (a) correlation coefficient of the relationship between net methane flux ($CH_4$ flux) and GPP at the diurnal scale in the different stages of growing season. (b) correlation coefficient of the relationship between $CH_4$ flux and soil temperature (Ts) at the diurnal scale in the different stages of growing season. The lag time corresponded with the largest absolute value of the correlation coefficient in each growing stage.

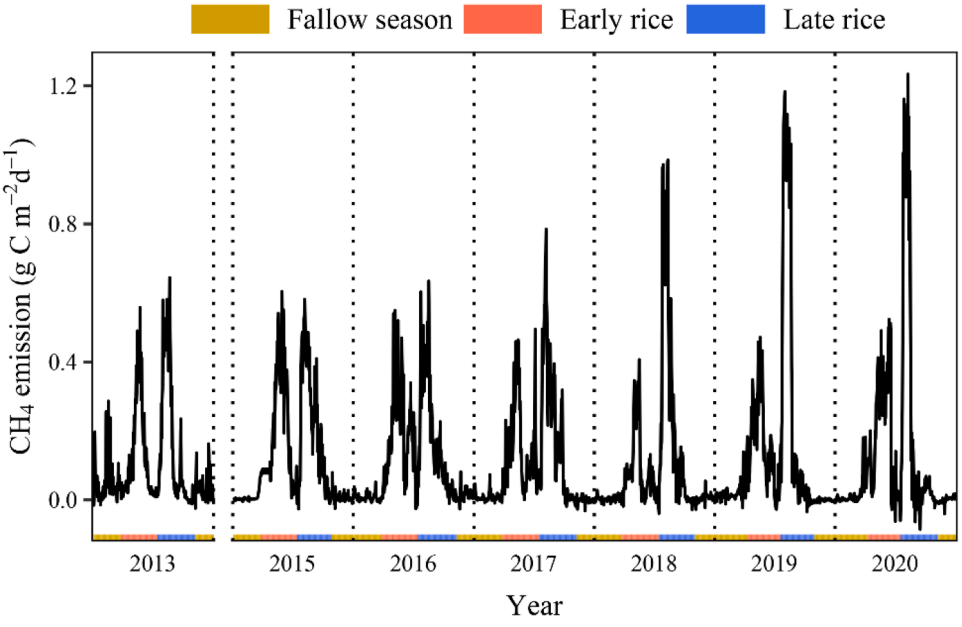


**Fig. 3.** Time series of daily $CH_4$ flux for early rice (red), late rice(blue) and fallow season (yellow) in 2013, 2015–2020.By the Random Forest analysis, 39–75% of $CH_4$ flux variation in the growing season could be explained by plant and environmental factors (Table 3). Soil moisture, GPP, *Re*, air pressure, and Ts were the most important driving forces in the growing season, and soil moisture dominated $CH_4$ emissions in the fallow season. At the seedling stage of early rice, Ts was the most important driving force of $CH_4$ flux. $CH_4$ flux was primarily driven by soil moisture during the booting and ripening stages. At the fallow season, $CH_4$ flux was only significantly affected by soil moisture. There was no significant effect of wind speed on $CH_4$ flux.

significantly increased with GPP, Ts, and decreased with air pressure (Fig. 4). Unlike previous studies, $CH_4$ flux increased with GPP following a logarithmic function (Fig. 4a). An exponential function was used to describe the Ts dependence of $CH_4$ flux (Fig. 4d). In addition, there was a simple linear relationship between $CH_4$ flux and air pressure (Fig. 4g). The relationship between $CH_4$ flux and soil moisture could be expressed as an exponential function during the booting and ripening stage (Fig. 4k and 4l).

The AIC value was used to compare the precision of the relationship between $CH_4$ flux and GPP at the vegetative stage using three different models (linear, exponential, logarithmic). Half of the results about the relationship between $CH_4$ flux and GPP in late rice did not differ using the different models ($\Delta AIC < 2$) when one-year or two-year data were used, whereas when using three-year or more data, the logarithmic model was optimal. A similar result was also obtained for early rice. The AIC values of the models were respectively −753, −681, and −822 for early rice, and −20, −15, and −29 for late rice based on seven-year data. Consequently, the relationship between $CH_4$ flux and GPP would be the

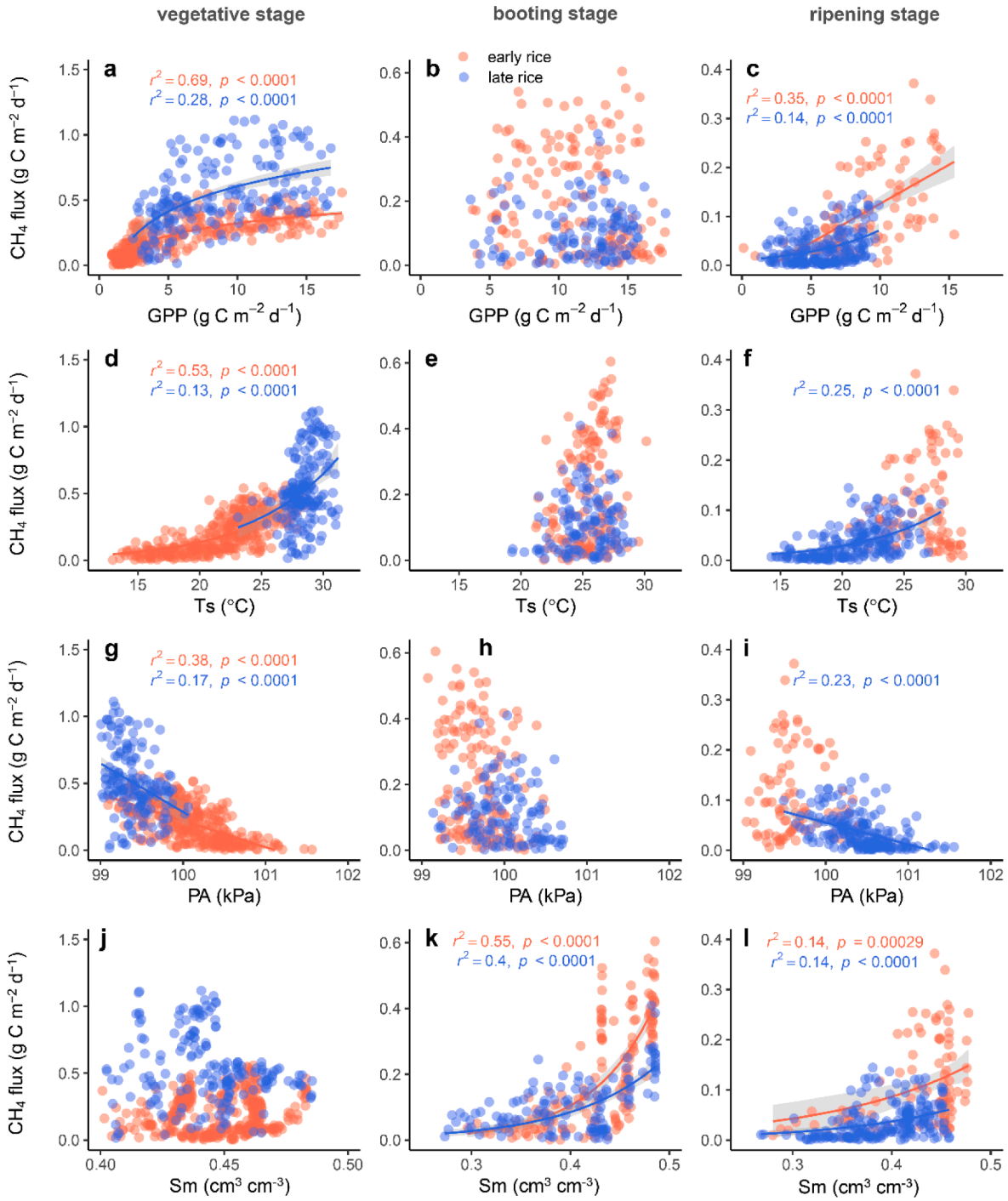


**Fig. 4.** The relationships between daily $CH_4$ flux and(a-c) GPP, (d-f) Ts, (g-i) air pressure (PA), and (j-l) soil moisture (Sm) during the (a, d, g, j) vegetative stage, (b, e, h, k) booting stage, and (c, f, i, l) ripening stage of early rice (red) and late rice (blue) from 2013 to 2020. The data during the period of flooding show logarithmic dependence on daily GPP of $CH_4$ emissions in Fig. 4a. Note the difference in the horizontal axis in Fig 4j compared with Fig 4k and 4i and the vertical axis in different stage.

best fit for a logarithmic model when three-year or more data applied.

### 3.3. Annual $CH_4$ emissions of double rice paddy

The annual $CH_4$ emissions of rice paddy were 42 ± 2 g C $m^{-2}$, ranging from 36 to 49 g C $m^{-2}$ over the seven years (Fig. 5). The $CH_4$ emissions accounted for 85.7–98% of the annual emissions during the growing season, in which early rice and late rice accounted for 40% and 55% on average, respectively. The average annual yield-scaled $CH_4$ emission was 32 g C $kg^{-1}$. The annual $CH_4$ emissions during the growing season exhibited a significant linear dependence on Ts (Fig. 6a, $r^2$ = 0.72). However, their relationships were poor in the fallow season. The $CH_4$ emissions during the fallow season of 2013 were much higher than those in other years (Fig. 5 and Fig. S3b). We found that the soil moisture was close to saturation during the fallow season in 2013 owing to dam leakage in the reservoir. The anaerobic soil environment favored the production of $CH_4$ (Fig. 5 and S3b). To avoid abnormal disturbances, we excluded the fallow season data from 2013 (Fig 6b), and reanalyzed the $CH_4$ emission-Ts relationship with the rest data. It was found that the annual $CH_4$ emissions during the fallow season also exhibited a significant linear dependence on Ts (Fig. 6b, $r^2$ = 0.68).

## 4. Discussion

### 4.1. Dominant driving forces of $CH_4$ flux at diurnal scale

Net $CH_4$ fluxes are largely controlled by simultaneous microbial production and oxidation, and the transport from soil to the atmosphere (Alberto et al., 2014). Any factors influencing these processes will affect $CH_4$ flux and their trends. At the diurnal scale, GPP, LE and Ts were dominant drivers or correlates of $CH_4$ flux (Table 2). By increasing GPP, more carbon substrates are provided for methanogenic metabolism, resulting in higher $CH_4$ production. $^{14}C$-labeling studies have also shown that $CH_4$ production is fueled by recent plant photosynthesis in the form of root exudates in the rhizosphere (Dorodnikov et al., 2011). GPP reached its peak earlier than $CH_4$ flux, which may have been caused by the unmatched transport time between the recently assimilated C allocation to belowground and $CH_4$ gas from the soil to the atmosphere (Mitra et al., 2020; Rinne et al., 2018; Swain et al., 2018). In our study, the lag time for diurnal GPP and $CH_4$ flux in the growing season changed at different growth stages because of the rate of carbohydrate transport throughout the plant (Thompson and Holbrook, 2003) and the development of plant aeration tissue.

There was also an association between $CH_4$ flux and LE (Fig. S1, Table 2). Because water evaporation and $CH_4$ volatilization from water and plant surfaces are driven by similar physical mechanisms, LE is unlikely to have a direct influence on $CH_4$ flux (Knox et al., 2020). LE could represent a proxy for $CH_4$ transport through the aerial tissue of rice plants. During the booting and ripening stages of early rice and late rice, rice plants did not limit $CH_4$ transport (Zhang et al., 2015) because of their well-developed aerenchyma system. As a result, the influence of LE on $CH_4$ flux decreased (Table 2).

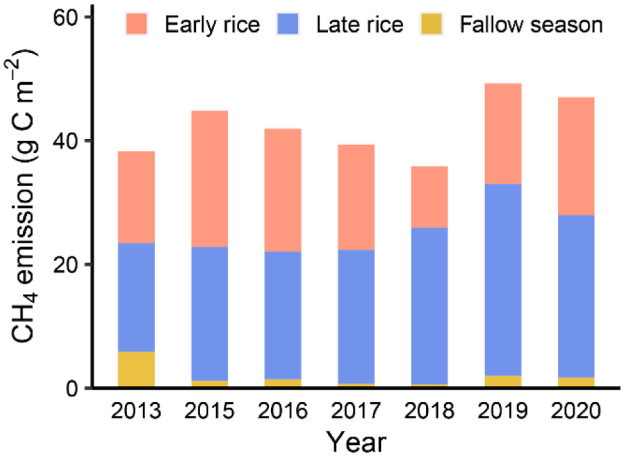


**Fig. 5.** Annual cumulative $CH_4$ flux and the emissions during the growing season of early rice (red), late rice (blue), and fallow season (yellow) in 2013, 2015–2020.

A higher Ts causes higher methanogenic bacteria activity and molecular diffusion (Hendriks et al., 2007; Sass et al., 1991; Swain et al., 2018). Although the rates of both $CH_4$ anaerobic oxidation (AOM) and methanogenesis increased with temperature, the rate of AOM was lower than that of methanogenesis in a $^{13}CH_4$ labeling experiment (Fan et al., 2021). The lag correlations between $CH_4$ flux and Ts were significant ($p < 0.05$) with lag times of 2.1 ± 0.4 h which changed in different stages (Fig. 2). Hysteresis of $CH_4$ flux and its variation during different growth stages have also been observed in freshwater wetlands (Liu et al., 2022).

A similar pattern was observed for the diurnal biophysical controls (except for soil moisture) with $CH_4$ flux, especially during the growing season. On the diurnal scale, soil moisture remained nearly unchanged, with a coefficient of variation (CV) ranging from 0.2% to 1.7%. So, soil moisture variations had no impact on change in $CH_4$ flux. With the drainage of paddy fields during the fallow stages, $CH_4$ flux greatly decreased (Iwata et al., 2018) because the aerobic environment did not favor methanogenic microbe but increased $CH_4$ oxidation.

### 4.2. Dominant driving forces of $CH_4$ flux at seasonal scale

The variation in $CH_4$ was greater during the growing season than that during the fallow season, showing a clear seasonal pattern (Fig. 3). A more pronounced temporal variation in $CH_4$ flux was found in late rice than in early rice. The mean soil temperature during the seedling and tillering stage was 21.5 °C in early rice and 28.2 °C in late rice. The highest $CH_4$ emissions emerged earlier in late rice (Fig. 3), for $CH_4$ emission of early rice peaked at 0.51 g C $m^{-2}$ $d^{-1}$ on the 54th day after planting, whereas late rice emission peaked at 0.86 g C $m^{-2}$ $d^{-1}$ on the 26th day after planting according to the 7-year average. It was due to the higher temperatures accelerated residue decomposition (Tang et al., 2014; Tokida et al., 2011) and the differences in management methods (direct-seeded culture for early rice and seedling-transplanted culture for late rice).

Many studies have indicated that $CH_4$ flux was mainly controlled by GPP (Dai et al., 2019; Li et al., 2021; Mitra et al., 2020). Therefore, the GPP of rice paddies is typically used as a predictor of $CH_4$ emissions in process models (Kettunen, 2003; Mi et al., 2014; Oikawa et al., 2017; Ueyama et al., 2022). However, the relationship between $CH_4$ emissions and GPP remains uncertain with linear or exponential relationships (Dai et al., 2019; Li et al., 2019; Song et al., 2015). This indicates that $CH_4$ emissions increase with increasing GPP in a stable or accelerated manner (Ge et al., 2018; Li et al., 2021). However, our study found that the relationship between $CH_4$ flux and GPP followed a logarithmic trend during the growing season under flooding conditions in both early rice and late rice (Fig. 6a). $CH_4$ emissions will not always increase with GPP but will be restricted to a maximum limit, which is quite different from previous studies. This result is important for precise evaluation of $CH_4$ emissions in large-scale modeling.

Some possible reasons have been proposed to explain the relationship between $CH_4$ flux and GPP in our study. First, GPP is distributed underground through the roots and is secreted into the soil as root exudates, providing organic matter for methanogens. There is evidence that the organic matter content in the soil first increases and then decreases on a daily timescale as GPP grows, and the organic matter allocated to the soil by GPP gradually decreases (Kimura et al., 2004). In this case, $CH_4$ emissions may reach a threshold as GPP grows rather than continue to grow. Second, elevated GPP could cause increased root porosity and root biomass, and as a result, methanotrophic activity is

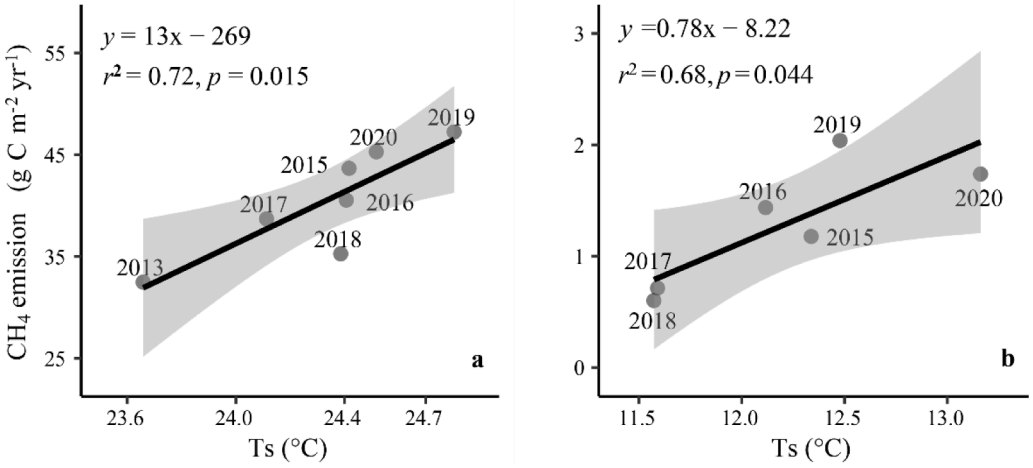


**Fig. 6.** The relationship between annual $CH_4$ emissions and mean Ts during the (a) growing season, and (b) fallow season.

stimulated (Jiang et al., 2017; Ma et al., 2010). Larger and more porous root system promotes the oxidation of $CH_4$ by transporting more $O_2$ into the soil. Hence, $CH_4$ emissions may stabilize as GPP increases. Third, using linear, exponential, and logarithmic models, we analyzed the relationship between $CH_4$ and GPP in late rice and found that when using one-year or two-year data, half of the results did not differ between the three models (AIC $<$ 2), whereas when using data of three years or more, the logarithmic model was optimal. Long-term data ($>$ 3 years) have been shown to stabilize the model for $CH_4$ flux simulations (Ueyama et al., 2022). The lack of appropriate treatment or important processes may lead to incorrect conclusions (Knox et al., 2016). Studies conducted over long periods of time can reveal insights that are difficult to reveal in short-term studies owing to the natural variability of the variables (Hanson and Walker, 2020). As a result, the logarithmic relationship between $CH_4$ flux and GPP in long-term observation (7-year) may be more reasonable compared to the studies those found a linear or exponential relationship using one- or two-year data (Dai et al., 2019; Ge et al., 2018; Li et al., 2019).

### 4.3. Annual variation in $CH_4$ emissions

The annual $CH_4$ emissions were 42 ± 2 g C $m^{-2}$ with a CV of 12%. The emissions strengths were the same as those of rice-wheat rotation system with annual emissions ranging from 37 to 49 g C $m^{-2}$ (Li et al., 2019, 2021). Lower $CH_4$ emissions were also found in rice paddies, with annual $CH_4$ emissions of the growing season was 19 g C $m^{-2}$(Ge et al., 2018) and 29 g C $m^{-2}$(Ma et al., 2021). In other regions, annual $CH_4$ emissions from rice paddies range from 6 to 22 g C $m^{-2}$(Alberto et al., 2015; Hwang et al., 2020; Knox et al., 2016; Runkle et al., 2019). The annual $CH_4$ emissions in this study were relatively high compared to other studies using the eddy covariance method. This was probably because the double cropping rice was planted in our study with longer growing period which produced greater $CH_4$ emissions than the single cropping rice (Feng et al., 2013). We also compared the yield-scaled $CH_4$ emissions of different rice cropping systems and found that the yield-scaled $CH_4$ emissions were also relatively high at our study site. The yield-scaled $CH_4$ emissions generally ranged from 6 g C $kg^{-1}$ to 37 g C $kg^{-1}$ using the eddy covariance method (Hwang et al., 2020; Knox et al., 2016; Runkle et al., 2019; Shi et al., 2023). While it was 32 g C $kg^{-1}$ at our site in this study and slightly lower than 37 g C $kg^{-1}$ rice at Nanchang Site, another double cropping rice planting site in this region (Shi et al., 2023), and it was in the high range for single cropping rice planting sites with yield-scaled $CH_4$ emissions ranging from 6 g C $kg^{-1}$ to 34 g C $kg^{-1}$ (Hwang et al., 2020; Knox et al., 2016; Runkle et al., 2019). So, the local environment in subtropical region may also contribute to the high $CH_4$ emissions to some extent (Turetsky et al., 2014).

At the annual scale, GPP had an insignificant effect on $CH_4$ emissions. Kuhn et al. (2021) found that $CH_4$ flux from terrestrial ecosystems was primarily influenced by GPP on the annual scale and was logarithmically related to GPP. Using a space-for-time analog, $CH_4$ flux and GPP may have the same relationship over a long time series. This may be because the rice paddies are intensively managed using the same plant species and agricultural management practices. This may have a similar biological influence on $CH_4$ production, oxidation, and transportation each year, resulting in smaller interannual changes in $CH_4$ emissions. More long-term data are required to estimate the interannual relationship between $CH_4$ emissions and GPP. Ts was identified as the dominant environmental factor affecting $CH_4$ flux on annual scale during the growing season and fallow season (Fig. 6). This was consistent with expectations, as many studies have indicated that annual $CH_4$ emissions of wetland ecosystems were also temperature-dependent (Knox et al., 2019; Ueyama et al., 2023; Yvon-Durocher et al., 2014) . In this region, $CH_4$ emissions could provide positive feedback regarding climate warming.

## Conclusions

Double rice cropping systems are widely distributed in Southern China. Rice paddies are among the most important $CH_4$ sources in terrestrial ecosystems. In this study, the annual $CH_4$ emissions were estimated at 42 ± 2 g C $m^{-2}$ with a CV of 12% in a double-rice cropping system using 7 years of flux data in Southern China. GPP had an insignificant effect on annual $CH_4$ emissions in this study. The dominant driving forces were analyzed, which indicated that soil temperature was the dominant environmental driving force affecting the interannual variation in $CH_4$ emissions from rice paddy during both the growing and fallow seasons. Thus, climate warming with increasing soil temperatures will probably cause higher annual $CH_4$ emissions from double-rice cropping system in this region. We found that the peak $CH_4$ flux in a day generally appeared at dusk during the vigorous growing period, which was quite different from the GPP peak at around noon. On seasonal time scale, daily $CH_4$ emissions showed a logarithmic relationship with GPP during the growing season of flooding conditions, which was quite different from previous results of linear or exponential relationships obtained using the observation data from one or two years. The $CH_4$-GPP relationship is very important and is usually used to evaluate $CH_4$ emissions from rice paddy in some models. Our findings imply that $CH_4$ emissions will not increase with increasing GPP in a stable or accelerating manner and that an upper limit of $CH_4$ emission exists. This is reasonable when considering plant growth and photosynthetic carbohydrate allocation patterns. This is important to improve the precision of estimating $CH_4$ emissions from rice paddies. The discrepancy in

the $CH_4$-GPP relationships between our study and previous studies may be partly ascribed to the data observation period. A $CH_4$-GPP relationship based on long-term observations is more reliable.

## Declaration of Competing Interest

The authors declare that they have no known competing financial interests or personal relationships that could have appeared to influence the work reported in this paper.

## Data availability

Data will be made available on request.

## Acknowledgments

This study was funded by the National Natural Science Foundation of China (41830860). We thank Yuanfen Huang and Shanyuan Yin for their assistance in farmland management.

## Supplementary materials

Supplementary material associated with this article can be found, in the online version, at doi:10.1016/j.agrformet.2023.109578.

## References

Alberto, M.C.R., et al., 2014. Measuring methane flux from irrigated rice fields by eddy covariance method using open-path gas analyzer. Field Crops Res. 160, 12–21.
Alberto, M.C.R., et al., 2015. Straw incorporated after mechanized harvesting of irrigated rice affects net emissions of $CH_4$ and $CO_2$ based on eddy covariance measurements. Field Crops Res. 184, 162–175.
Baldocchi, D., Sturtevant, C., Fluxnet, C., 2015. Does day and night sampling reduce spurious correlation between canopy photosynthesis and ecosystem respiration? Agric. For. Meteorol. 207, 117–126.
Bhattacharyya, P., et al., 2019. Mechanism of plant mediated methane emission in tropical lowland rice. Sci. Total Environ. 651, 84–92.
Chaichana, N., et al., 2018. Comparison of closed chamber and eddy covariance methods to improve the understanding of methane fluxes from rice paddy fields in Japan. Atmosphere (Basel) 9 (9), 356.
Chen, W., et al., 2020. Hysteretic relationship between plant productivity and methane uptake in an alpine meadow. Agric. For. Meteorol. 288-289, 107982.
Chen, W., et al., 2019. Diel and seasonal dynamics of ecosystem-scale methane flux and their determinants in an alpine meadow. J. Geophys. Res.: Biogeosci. 124 (6), 1731–1745.
Chen, Z., Zhang, H., Xue, J., Liu, S., Chen, F., 2021. A nine-year study on the effects of tillage on net annual global warming potential in double rice-cropping systems in Southern China. Soil Tillage Res. 206, 104797.
Conrad, R., 2002. Control of microbial methane production in wetland rice fields. Nutr. Cycling Agroecosyst. 64 (1–2), 59–69.
Dai, S., et al., 2019. Variations and drivers of methane fluxes from a rice-wheat rotation agroecosystem in eastern China at seasonal and diurnal scales. Sci. Total Environ. 690, 973–990.
Dai, X., Yuan, Y., Wang, H., 2016. Changes of anaerobic to aerobic conditions but not of crop type induced bulk soil microbial community variation in the initial conversion of paddy soils to drained soils. Catena 147, 578–585.
Dorodnikov, M., Knorr, K.H., Kuzyakov, Y., Wilmking, M., 2011. Plant-mediated $CH_4$ transport and contribution of photosynthates to methanogenesis at a boreal mire: a $^{14}C$ pulse-labeling study. Biogeosciences 8 (8), 2365–2375.
Ehnes, R.B., Rall, B.C., Brose, U., 2011. Phylogenetic grouping, curvature and metabolic scaling in terrestrial invertebrates. Ecol. Lett. 14 (10), 993–1000.
Etheridge, D.M., Steele, L.P., Francey, R.J., Langenfelds, R.L., 1998. Atmospheric methane between 1000 AD and present: evidence of anthropogenic emissions and climatic variability. J. Geophys. Res.-Atmos. 103 (D13), 15979–15993.
Falge, E., et al., 2001. Gap filling strategies for defensible annual sums of net ecosystem exchange. Agric. For. Meteorol. 107 (1), 43–69.
FAO, 2020. FAOSTAT database. http://www.fao.org/faostat/en/#data/QC.
Fan, L., et al., 2021. Temperature sensitivity of anaerobic methane oxidation versus methanogenesis in paddy soil: implications for the $CH_4$ balance under global warming. Glob. Chang. Biol. 28 (2), 654–664.
Feng, J., et al., 2013. Impacts of cropping practices on yield-scaled greenhouse gas emissions from rice fields in China: a meta-analysis. Agric., Ecosyst. Environ. 164, 220–228.
Feng, Z.Y., Qin, T., Du, X.Z., Sheng, F., Li, C.F., 2021. Effects of irrigation regime and rice variety on greenhouse gas emissions and grain yields from paddy fields in central China. Agric. Water Manage. 250, 106830.
Ge, H.-X., et al., 2018. The characteristics of methane flux from an irrigated rice farm in East China measured using the eddy covariance method. Agric. For. Meteorol. 249, 228–238.
Hanson, P.J., Walker, A.P., 2020. Advancing global change biology through experimental manipulations: where have we been and where might we go? Glob. Chang. Biol. 26 (1), 287–299.
Hendriks, D.M.D., van Huissteden, J., Dolman, A.J., van der Molen, M.K., 2007. The full greenhouse gas balance of an abandoned peat meadow. Biogeosciences 4 (3), 411–424.
Hwang, Y., et al., 2020. Comprehensive assessments of carbon dynamics in an intermittently-irrigated rice paddy. Agric. For. Meteorol. 285-286, 107933.
IPCC, 2007. Climate Change 2007: The Physical Science Basis: Working Group I Contribution to the Fourth Assessment Report of the IPCC. Cambridge University Press.
Iwata, H., et al., 2018. Exploring sub-daily to seasonal variations in methane exchange in a single-crop rice paddy in central Japan. Atmos. Environ. 179, 156–165.
Jauhiainen, J., Takahashi, H., Heikkinen, J.E.P., Martikainen, P.J., Vasander, H., 2005. Carbon fluxes from a tropical peat swamp forest floor. Glob. Chang. Biol. 11 (10), 1788–1797.
Jiang, M., Xin, L., Li, X., Tan, M., Wang, R., 2018. Decreasing rice cropping intensity in southern China from 1990 to 2015. Rem. Sens. (Basel) 11 (1), 35.
Jiang, Y., et al., 2017. Higher yields and lower methane emissions with new rice cultivars. Glob. Chang. Biol. 23 (11), 4728–4738.
Kabacoff, R., 2015. R in Action: Data Analysis and Graphics with R. Manning Publications.
Kettunen, A., 2003. Connecting methane fluxes to vegetation cover and water table fluctuations at microsite level: a modeling study. Glob. Biogeochem. Cycles 17 (2), 1051.
Kim, Y., et al., 2016. Interannual variations in methane emission from an irrigated rice paddy caused by rainfalls during the aeration period. Agric. Ecosyst. Environ. 223, 67–75.
Kimura, M., Murase, J., Lu, Y., 2004. Carbon cycling in rice field ecosystems in the context of input, decomposition and translocation of organic materials and the fates of their end products ($CO_2$ and $CH_4$). Soil Biol. Biochem. 36 (9), 1399–1416.
Knox, S.H., et al., 2020. Identifying dominant environmental predictors of freshwater wetland methane fluxes across diurnal to seasonal time scales. Glob. Chang. Biol. 27, 3582–3604.
Knox, S.H., et al., 2019. FLUXNET-$CH_4$ synthesis activity: objectives, observations, and future directions. Bull. Am. Meteorol. Soc. 100 (12), 2607–2632.
Kljun, N., Calanca, P., Rotach, M.W., Schmid, H.P., 2004. A simple parameterisation for flux footprint predictions. Bound.-Layer Meteorol. 112 (3), 503–523.
Knox, S.H., et al., 2016. Biophysical controls on interannual variability in ecosystem-scale $CO_2$ and $CH_4$ exchange in a California rice paddy. J. Geophys. Res.: Biogeosci. 121 (3), 978–1001.
Kuhn, M.A., et al., 2021. BAWLD-$CH_4$: a comprehensive dataset of methane fluxes from boreal and arctic ecosystems. Earth Syst. Sci. Data 13 (11), 5151–5189.
Le Mer, J., Roger, P., 2001. Production, oxidation, emission and consumption of methane by soils: a review. Eur. J. Soil Biol. 37 (1), 25–50.
Leamer, E.E., 1985. Sensitivity analyses would help. Am. Econ. Rev. 75 (3), 308–313.
Li, H., et al., 2019. Does direct-seeded rice decrease ecosystem-scale methane emissions?—A case study from a rice paddy in southeast China. Agric. For. Meteorol. 272-273, 118–127.
Li, H., et al., 2021. Gross ecosystem productivity dominates the control of ecosystem methane. Land (Basel) 10 (11), 1186.
Li, J., et al., 2018. Combination of modified nitrogen fertilizers and water saving irrigation can reduce greenhouse gas emissions and increase rice yield. Geoderma 315, 1–10.
Liaw, A. and Wiener, M., 2002. Classification and regression by randomForest. R news, 2 (3): 18–22.
Liu, H., et al., 2021. Phenological mismatches between above- and belowground plant responses to climate warming. Nat. Clim. Chang. 12 (1), 97–102.
Liu, J., Valach, A., Baldocchi, D., Lai, D.Y.F., 2022. Biophysical controls of ecosystem-scale methane fluxes from a subtropical estuarine mangrove: multiscale, nonlinearity, asynchrony and causality. Glob. Biogeochem. Cycles 36 (6), e2021GB007179.
Lloyd, J., Taylor, J.A., 1994. On the temperature-dependence of soil respiration. Funct. Ecol. 8 (3), 315–323.
Ma, K.E., Qiu, Q., Lu, Y., 2010. Microbial mechanism for rice variety control on methane emission from rice field soil. Glob. Chang. Biol. 16 (11), 3085–3095.
Ma, L., Liu, B., Cui, Y., Shi, Y., 2021. Variations and drivers of methane fluxes from double-cropping paddy fields in southern China at diurnal, seasonal and inter-seasonal timescales. Water (Basel) 13 (16), 2171.
Maier, M., Mayer, S., Laemmel, T., 2019. Rain and wind affect chamber measurements. Agric. For. Meteorol. 279, 107754.
Massman, W.J., Lee, X., 2002. Eddy covariance flux corrections and uncertainties in long-term studies of carbon and energy exchanges. Agric. For. Meteorol. 113 (1–4), 121–144.
Meijide, A., Gruening, C., Goded, I., Seufert, G., Cescatti, A., 2017. Water management reduces greenhouse gas emissions in a Mediterranean rice paddy field. Agric., Ecosyst. Environ. 238, 168–178.
Mi, Y., et al., 2014. Improving a plot-scale methane emission model and its performance at a northeastern Siberian tundra site. Biogeosciences 11 (14), 3985–3999.
Mitra, B., et al., 2020. Spectral evidence for substrate availability rather than environmental control of methane emissions from a coastal forested wetland. Agric. For. Meteorol. 291, 108062.

Moncrieff, J., Clement, R., Finnigan, J., Meyers, T., 2004. Averaging, detrending, and filtering of eddy covariance time series. In: Handbook of Micrometeorology: A Guide For Surface Flux Measurement and Analysis, 29. Kluwer Academic Press, pp. 7–31.
Moncrieff, J.B., et al., 1997. A system to measure surface fluxes of momentum, sensible heat, water vapour and carbon dioxide. J. Hydrol. (Amst) 188 (1–4), 589–611.
Morin, T.H., 2019. Advances in the eddy covariance approach to $CH_4$ monitoring over two and a half decades. J. Geophys. Res.-Biogeosci. 124 (3), 453–460.
NBS, 2018. Annual agricultural data for China. https://data.stats.gov.cn/english/easyquery.htm?cn=C01.
Neue, H.U., 1993. Methane emission from rice fields. Bioscience 43 (7), 466–474.
Nisbet, E.G., et al., 2019. Very Strong Atmospheric Methane Growth in the 4 Years 2014–2017: implications for the Paris Agreement. Glob. Biogeochem. Cycles 33 (3), 318–342.
Oikawa, P.Y., et al., 2017. Evaluation of a hierarchy of models reveals importance of substrate limitation for predicting carbon dioxide and methane exchange in restored wetlands. J. Geophys. Res.-Biogeosci. 122 (1), 145–167.
Reba, M.L., Fong, B.N., Rijal, I., 2019. Fallow season $CO_2$ and $CH_4$ fluxes from US mid-south rice-waterfowl habitats. Agric. For. Meteorol. 279, 107709.
Rinne, J., et al., 2018. Temporal variation of ecosystem scale methane emission from a boreal fen in relation to temperature, water table position, and carbon dioxide fluxes. Glob. Biogeochem. Cycles 32 (7), 1087–1106.
Runkle, B.R.K., et al., 2019. Methane Emission Reductions from the Alternate Wetting and Drying of Rice Fields Detected Using the Eddy Covariance Method. Environ. Sci. Technol. 53 (2), 671–681.
Sass, R.L., Fisher, F.M., Turner, F.T., Jund, M.F., 1991. Methane emission from rice fields as influenced by solar radiation, temperature, and straw incorporation. Glob. Biogeochem. Cycles 5 (4), 335–350.
Shao, R., et al., 2017. Land use legacies and nitrogen fertilization affect methane emissions in the early years of rice field development. Nutr. Cycling Agroecosyst. 107 (3), 369–380.
Shi, Y.-Z., Cui, Y.-L., Cai, S., Hong, D.-L., Cheng, J., 2023. $CH_4$ Fluxes and their comprehensive greenhouse effects with $CO_2$ fluxes in direct-seeded rice in Poyang Lake Plain. Huan Jing Ke Xue 44 (3), 1572–1582.
Song, W., et al., 2015. Methane emissions from an alpine wetland on the Tibetan Plateau: neglected but vital contribution of the nongrowing season. J. Geophys. Res.: Biogeosci. 120 (8), 1475–1490.
Swain, C.K., et al., 2018. Greenhouse gas emissions and energy exchange in wet and dry season rice: eddy covariance-based approach. Environ. Monit. Assess. 190 (7), 423.
Tariq, A., Jensen, L.S., de Tourdonnet, S., Sander, B.O., de Neergaard, A., 2017a. Early drainage mitigates methane and nitrous oxide emissions from organically amended paddy soils. Geoderma 304, 49–58.
Tang, H.M., et al., 2014. Effects of winter cover crops straws incorporation on $CH_4$ and $N_2O$ emission from double-cropping paddy fields in southern China. Plos One 9 (10), e108322.
Tariq, A., et al., 2017b. Mitigating $CH_4$ and $N_2O$ emissions from intensive rice production systems in northern Vietnam: efficiency of drainage patterns in combination with rice residue incorporation. Agric. Ecosyst. Environ. 249, 101–111.
Thompson, M.V., Holbrook, N.M., 2003. Scaling phloem transport: water potential equilibrium and osmoregulatory flow. Plant Cell Environ. 26 (9), 1561–1577.
Tokida, T., et al., 2011. Methane and soil $CO_2$ production from current-season photosynthates in a rice paddy exposed to elevated $CO_2$ concentration and soil temperature. Glob. Chang. Biol. 17 (11), 3327–3337.
Turetsky, M.R., et al., 2014. A synthesis of methane emissions from 71 northern, temperate, and subtropical wetlands. Glob. Chang. Biol. 20 (7), 2183–2197.
Ueyama, M., et al., 2023. Modeled production, oxidation, and transport processes of wetland methane emissions in temperate, boreal, and Arctic regions. Glob. Chang. Biol. 29 (8), 2313–2334.
Ueyama, M., Yazaki, T., Hirano, T., Endo, R., 2022. Partitioning methane flux by the eddy covariance method in a cool temperate bog based on a Bayesian framework. Agric. For. Meteorol. 316, 108852.
Van Dijk, A.I.J.M., Han Dolman, A.J., 2004. Estimates of $CO_2$ uptake and release among European forests based on eddy covariance data. Glob. Chang. Biol. 10 (9), 1445–1459.
Verma, S.B., et al., 1992. Eddy-correlation measurements of methane flux in a northern peatland ecosystem. Boundary Layer Meteorol. 58 (3), 289–304.
Wang, B., et al., 2016. Modifying nitrogen fertilizer practices can reduce greenhouse gas emissions from a Chinese double rice cropping system. Agriculture. Ecosyst. Environ. 215, 100–109.
Wang, C., et al., 2019. Responses of greenhouse-gas emissions to land-use change from rice to jasmine production in subtropical China. Atmos. Environ. 201, 391–401.
Wassmann, R., Aulakh, M.S., 2000. The role of rice plants in regulating mechanisms of methane missions. Biol. Fertil. Soils 31 (1), 20–29.
Webb, E.K., Pearman, G.I., Leuning, R., 1980. Correction of flux measurements for density effects due to heat and water-vapor transfer. Q. J. R. Meteorolog. Soc. 106 (447), 85–100.
Yang, Y., et al., 2018. Winter tillage with the incorporation of stubble reduces the net global warming potential and greenhouse gas intensity of double-cropping rice fields. Soil Tillage Res. 183, 19–27.
Yu, K., et al., 2021. Low greenhouse gases emissions associated with high nitrogen use efficiency under optimized fertilization regimes in double-rice cropping systems. Appl. Soil Ecol. 160, 103846.
Yu, L., et al., 2013. A comparison of methane emission measurements using Eddy Covariance and manual and automated chamber-based techniques in Tibetan Plateau alpine wetland. Environ. Pollut. 181, 81–90.
Yuan, Y., et al., 2016. Effects of land-use conversion from double rice cropping to vegetables on methane and nitrous oxide fluxes in southern China. PLoS ONE 11 (5), e0155926.
Yvon-Durocher, G., et al., 2014. Methane fluxes show consistent temperature dependence across microbial to ecosystem scales. Nature 507 (7493), 488–491.
Zhang, Y., et al., 2015. Aboveground morphological traits do not predict rice variety effects on $CH_4$ emissions. Agric. Ecosyst. Environ. 208, 86–93.
Zhao, J., et al., 2019. An evaluation of the flux-gradient and the eddy covariance method to measure $CH_4$, $CO_2$, and $H_2O$ fluxes from small ponds. Agric. For. Meteorol. 275, 255–264.